



# Environmental mobility of $^{110m}\text{Ag}$ : lessons learnt from Fukushima accident (Japan) and potential use for tracking the dispersion of contamination within coastal catchments

Hugo Lepage, O. Evrard, Yuichi Onda, Jérémie Patin, Caroline Chartin, Irène Lefevre, Philippe Bonté, Sophie Ayrault

## ► To cite this version:

Hugo Lepage, O. Evrard, Yuichi Onda, Jérémie Patin, Caroline Chartin, et al.. Environmental mobility of  $^{110m}\text{Ag}$ : lessons learnt from Fukushima accident (Japan) and potential use for tracking the dispersion of contamination within coastal catchments. *Journal of Environmental Radioactivity*, 2014, 130, pp.44-55. 10.1016/j.jenvrad.2013.12.011 . cea-02614715

HAL Id: cea-02614715

<https://cea.hal.science/cea-02614715>

Submitted on 25 May 2020

**HAL** is a multi-disciplinary open access archive for the deposit and dissemination of scientific research documents, whether they are published or not. The documents may come from teaching and research institutions in France or abroad, or from public or private research centers.

L'archive ouverte pluridisciplinaire **HAL**, est destinée au dépôt et à la diffusion de documents scientifiques de niveau recherche, publiés ou non, émanant des établissements d'enseignement et de recherche français ou étrangers, des laboratoires publics ou privés.

**Environmental mobility of  $^{110m}\text{Ag}$ : lessons learnt from Fukushima accident  
(Japan) and potential use for tracking the dispersion of contamination within  
coastal catchments**

**Hugo Lepage<sup>a,\*</sup>, Olivier Evrard<sup>a</sup>, Yuichi Onda<sup>b</sup>, Jeremy Patin<sup>b</sup>, Caroline Chartin<sup>a</sup>, Irène  
Lefèvre<sup>a</sup>, Philippe Bonté<sup>a</sup>, Sophie Ayrault<sup>a</sup>**

<sup>a</sup> Laboratoire des Sciences du Climat et de l'Environnement (LSCE/IPSL), Unité Mixte de  
Recherche 8212 (CEA, CNRS, UVSQ), 91198, Gif-sur-Yvette Cedex, France

<sup>b</sup> Center for Research in Isotopes and Environmental Dynamics (CRIED), University of  
Tsukuba, 1-1-1 Tennodai, Tsukuba, Ibaraki 305-8572, Japan

\* Corresponding author.

E-mail address: [hugo.lepage@lsce.ipsl.fr](mailto:hugo.lepage@lsce.ipsl.fr) (H. Lepage).

Telephone: +33/1/69.82.43.33

1   **Environmental mobility of  $^{110m}\text{Ag}$ : lessons learnt from Fukushima accident**

2   **(Japan) and potential use for tracking the dispersion of contamination within**

3   **coastal catchments**

4

5   **Abstract**

6   Silver-110 metastable ( $^{110m}\text{Ag}$ ) has been far less investigated than other anthropogenic  
7   radionuclides, although it has the potential to accumulate in plants and animal tissues. It is  
8   continuously produced by nuclear power plants in normal conditions, but emitted in much  
9   larger quantities in accidental conditions facilitating its detection, which allows the  
10   investigation of its behaviour in the environment. We analysed  $^{110m}\text{Ag}$  in soil and river drape  
11   sediment (i.e., mud drapes deposited on channel-bed sand) collected within coastal  
12   catchments contaminated in Fukushima Prefecture (Japan) after the Fukushima Dai-ichi  
13   Nuclear Power Plant accident that occurred on 11 March 2011. Several field experiments  
14   were conducted to document radiosilver behaviour in the terrestrial environment, with a  
15   systematic comparison to the more documented radiocesium behaviour. Results show a  
16   similar and low mobility for both elements in soils and a strong affinity with the clay fraction.  
17   Measurements conducted on sediment sequences accumulated in reservoirs tend to confirm  
18   a comparable migration and deposition of those radionuclides even after their redistribution  
19   due to erosion and deposition processes. Therefore, as the  $^{110m}\text{Ag}:\text{Cs}^{137}$  initial activity ratio  
20   varied in soils across the area, we justified the relevance of using this tool to track the  
21   dispersion of contaminated sediment from the main inland radioactive pollution plume  
22   generated by FDNPP accident.

23        **1. Introduction**

24        Silver-110 metastable ( $^{110m}\text{Ag}$ ) is a radioisotope with a rather short half-life of 249 days  
25        produced in nuclear power plants (NPP) as an activation product of  $^{109}\text{Ag}$ . In NPP, natural  
26        silver (which contains 48% of  $^{109}\text{Ag}$ ) is found in control rods or in the alloy used to seal the  
27        head of the reactor (-Calmon and Garnier-Laplace 2002; Chelet 2006; IAEA 1998). In addition,  
28         $^{109}\text{Ag}$  may also be a fission product from uranium and plutonium (Chelet, 2006).  $^{110m}\text{Ag}$  can  
29        be measured by spectrometry gamma (with the main peak at 658 keV, and secondary peaks  
30        at 885 and 937 keV).

31        Le Petit et al. (2012) described the  $^{110m}\text{Ag}$  as a volatile fuel particle displaying some common  
32        characteristics with semi-volatile substances, due to its well-known strong retention within  
33        the reactor core structures. Even though  $^{110m}\text{Ag}$  is produced by NPP in normal operational  
34        conditions, its release into the environment remains limited (Ciffroy et al., 2005; Eyrolle et  
35        al., 2012) (Table 1), and research on this radionuclide has mainly gained interest after  
36        Chernobyl and Fukushima Dai-ichi accidents when it was emitted in much larger quantities,  
37        which facilitated its measurement. A search of the Web of Knowledge citation index (July  
38        2013) shows that the number of publications about  $^{110m}\text{Ag}$  increased significantly after  
39        Chernobyl accident (Fig. 1). A similar increase in attention has already been observed shortly  
40        after Fukushima accident.

41        Few information are available on the environmental mobility of  $^{110m}\text{Ag}$ , and most of the  
42        studies regarding this radioisotope were conducted in laboratory (Calmon and Garnier-  
43        Laplace 2002) because the conditions necessary to conduct field experiments were rarely  
44        met, as samples should be collected within the months following a release. They should  
45        alternatively be recovered in large quantities and analysed with high sensitivity detectors

46 during relatively long counting times. Still, it remains important to better understand its  
47 behaviour in the environment, as it has been demonstrated that silver is one of the most  
48 toxic metals (Bryan, 1971; Ratte, 1999) and that  $^{110m}\text{Ag}$  may be transferred from the soils to  
49 the plants (Handl et al., 2000; Shang and Leung, 2003), and accumulated in animal tissues  
50 (Adam et al., 2001; Beresford et al., 1998; Bryan and Langston, 1992; Khangarot and Ray,  
51 1987; Martin and Holdich, 1986; Oughton, 1989). It can also contaminate natural silver  
52 (isotopic contamination) used for photographic industry and jewellery manufacturing  
53 (Vuković, 2002).

54 Besides this interest to better understand the radioecology of  $^{110m}\text{Ag}$ , it has been shown that  
55 this radioisotope was emitted by the Fukushima Dai-ichi Nuclear Power Plant (FDNPP)  
56 accident and subsequently detected in the environment (Fukuda et al., 2013; MEXT, 2011;  
57 Tazoe et al., 2012; Watanabe et al., 2012). It is estimated that 20% of the radionuclides  
58 emitted were deposited on the soils of Fukushima Prefecture as a result of wet and dry  
59 atmospheric fallout, creating a contamination plume extending up to 70 km to the  
60 northwest of the FDNPP site (Kinoshita et al., 2011; Yasunari et al., 2011). It was estimated  
61 that between 7 and 36 PBq of  $^{137}\text{Cs}$  ( $T_{1/2} = 30.17\text{y}$ ) were released (Chino et al., 2011; Stohl et  
62 al., 2012; Winiarek et al., 2012), and  $^{110m}\text{Ag}$  release rate represented about 11% of the  $^{137}\text{Cs}$   
63 rate (Petit et al., 2012).

64 Depending on the behaviour of the radionuclides and their affinity with the fine mineral  
65 particles and the associated organic matter fraction, they may subsequently be redistributed  
66 across hillslopes as a consequence of runoff and soil erosion processes and be delivered to  
67 downstream rivers that may finally supply them to the ocean (Tanaka et al., 2012; Tateda et  
68 al., 2013; Ueda et al., 2013). Even though the bulk of initial marine contamination originated

69 from atmospheric deposition, erosion processes may have partly supplied the  $^{110m}\text{Ag}$  that  
70 was detected in zooplankton in the Pacific Ocean shortly after the accident (Buesseler et al.,  
71 2012).

72 In order to document this transfer, Chartin et al. (2013) showed that the spatial patterns of  
73  $^{110m}\text{Ag}:\text{Cs}$  activity ratio in soils varied across space within the Fukushima contamination  
74 plume. They subsequently used this ratio to track the dispersion of contaminated sediment  
75 along a coastal river draining a catchment located within the main radioactive plume.

76 However, to date, most studies conducted in Fukushima post-accidental conditions focused  
77 on  $^{134}\text{Cs}$  and  $^{137}\text{Cs}$  behaviour (Inoue et al. 2013; Koarashi et al. 2012; Kato et al. 2012a,  
78 2012b; Matsunaga et al. 2013). Investigations reporting the presence of  $^{110m}\text{Ag}$  in soil did not  
79 detail its distribution with depth nor its behaviour (Fukuda et al., 2013; Tazoe et al., 2012;  
80 Watanabe et al., 2012). In this context, there is a lack of data collected in this specific post-  
81 accidental context to document the relative behaviour of  $^{110m}\text{Ag}$  and  $^{137}\text{Cs}$  in soils and  
82 sediment in order to check the relevance of using this ratio to track the dispersion of  
83 contaminated material along rivers. Even though both radionuclides are particle-reactive,  
84 the  $^{110m}\text{Ag}:\text{Cs}$  activity ratio in mobilized sediment might not simply reflect the catchment  
85 soil average of this ratio.

86 In this context, this paper aims to compile original experimental data acquired in Fukushima  
87 Prefecture during the months that followed the accident to document  $^{110m}\text{Ag}$  behaviour in  
88 soils and sediment. This paper will particularly address four issues:

89 (1) the affinity of  $^{110m}\text{Ag}$  with different grain size fractions, to check whether there is a  
90 different behaviour of  $^{110m}\text{Ag}$  and  $^{137}\text{Cs}$  depending on the particle size;  
91 (2) the migration of  $^{110m}\text{Ag}$  in the soil, to investigate its potential movement with depth;

92 (3) the evolution of  $^{110m}\text{Ag}$  activities within sediment sequences accumulated in  
93 reservoirs, to document whether characteristics of contaminated sediments  
94 delivered to the reservoir by successive flood events change with time;  
95 (4) the evolution of  $^{110m}\text{Ag}$  activities within sediment drape deposits, that consist of mud  
96 drapes deposited on channel-bed sand (Olley et al., 2013), collected at the same  
97 locations along the rivers after a succession of typhoon and snowmelt events to  
98 investigate the impact of those events on  $^{110m}\text{Ag}$  redistribution in catchments.

99 We will systematically compare the radiosilver behaviour to the one of the well documented  
100 radiocaesium, and to the literature data. The implications of those results will finally be  
101 discussed to decide whether the use of the  $^{110m}\text{Ag} : ^{137}\text{Cs}$  activity ratio is relevant to track the  
102 dispersion of contaminated sediment from the main radioactive pollution plume generated  
103 by FDNPP accident.

## 104 **2. Materials and methods**

### 105 2.1. Study area

106 The study was conducted in Fukushima Prefecture, located in Northeastern Japan. We  
107 focused on several coastal catchments (i.e. Mano, Nitta, Ota and Odaka catchments) (1000  
108 km<sup>2</sup>) draining the main part of the radioactive plume extending to the northwest of FDNPP  
109 (Fig. 2). Those catchments extend from the coastal mountain range (at approximately 30-km  
110 distance of the coast) to the Pacific Ocean and their elevation ranges from 0 to 900 m.

111 Plateaus on the west consist of Cretaceous granite and granodiorite, evolving into a complex  
112 patchwork of volcanic (both intrusive and extrusive), metamorphic (gneiss and schist) and  
113 plutonic (granite mainly) rocks. In the middle part of the catchments, marine and continental

114 sedimentary rocks of various ages separated by fault systems are found. In contrast, eastern  
115 coastal plains are mainly composed of Tertiary and Quaternary marine and continental  
116 sedimentary rocks.

117 Woodland is the main land use in this area (covering 68–78% of the total surface), followed  
118 by cropland (10–13%). The region is exposed to typhoons and spring snowmelt events  
119 leading to severe soil erosion and subsequent export of sediment in rivers (Chartin et al.,  
120 2013; Evrard et al., 2013). We therefore conducted three sampling campaigns after each of  
121 those major hydro-sedimentary events (i.e., Nov. 2011, April 2012, and Nov. 2012).

122 2.2. Sample collection, preparation and description of experiments.

123 After the accident, the Ministry of Education, Culture, Sports, Science and Technology in  
124 Japan (MEXT) supervised the sampling of soils at 2200 sites located within a radius of  
125 approximately 100 km around FDNPP in June and July 2011, and the analysis of their  
126 activities in several radionuclides contained in their 5-cm upper layer ( $^{110m}\text{Ag}$  activities were  
127 only provided for a selection of 345 sites; MEXT 2011).

128 Based on this dataset, a map of  $^{110m}\text{Ag}:\text{Cs}^{137}$  activity ratio values in soils was drawn (Chartin  
129 et al., 2013). Unlike  $^{134}\text{Cs}:\text{Cs}^{137}$  activity ratio, it revealed the presence of different  
130 contamination patterns across the area (Fig. 3), with lower values across mountains and  
131 higher values in the coastal lowlands.

132 The relatively low abundance of  $^{110m}\text{Ag}$  in soils of the study area in Fukushima (activities  
133 ranging between 2 – 2400 Bq kg<sup>-1</sup>) compared to those in  $^{134}\text{Cs}$  and  $^{137}\text{Cs}$  (500 – 1,245,000 Bq  
134 kg<sup>-1</sup>) required relatively long counting times and the use of low-background high-resolution  
135 detectors to allow its detection. This probably explains why this radioisotope has not been

136 measured more widely during the months that followed the accident. We therefore decided  
137 to restrict this study to the main contamination plume (Table 2) in order to minimize  
138 uncertainties associated with  $^{110m}\text{Ag}$  measurements.

139       **A. Behaviour of  $^{110m}\text{Ag}$  in soils**

140       *Experiment 1 – Affinity with different grain size fractions*

141 Four soil samples (~300g/sample – Soil 1 to Soil 4 - Fig. 3) were collected using non-metallic  
142 trowels in different parts of the contamination plume where  $^{110m}\text{Ag} : ^{137}\text{Cs}$  activity ratio varies  
143 from 0.002 to 0.008. After drying at 40°C, samples were dry-sieved to 1mm, 500µm, 250µm  
144 and 63µm using an automatic device, in order to measure the respective activities present in  
145 the different grain size fractions.

146       *Experiment 2 – Migration in soil*

147 To investigate the potential migration of radionuclides with depth in soil, gamma  
148 measurements were conducted on each 2-mm increment of the uppermost 2-cm of a soil  
149 profile sampled near Kawamata city (Profile - Fig. 3). Soil layers were collected using a  
150 scraper plate composed by a metal frame and a metal plate (Loughran et al., 2002; Kato et  
151 al., 2012b). To avoid contamination by top layers, a spray glue was used to fix the sample.

152  $^{137}\text{Cs}$  concentration in undisturbed Japanese soils is expected to show an exponential decline  
153 with depth (Kato et al., 2012b; Koarashi et al., 2012; Matsunaga et al., 2013). Cumulative  
154 inventory can be expressed as described in Eq. (1):

$$155 \quad I_{(x)} = I_t (1 - \exp^{-x/h_0}) \quad (1)$$

156 Where  $I_{(x)}$  is the radiocesium inventory ( $\text{Bq.m}^{-2}$ ) at the  $x$  ( $\text{kg.m}^{-2}$ ) depth,  $I_t$  is the total  
157 radiocesium inventory and  $h_0$  is the relaxation mass depth ( $\text{kg.m}^2$ ), an index characterising  
158 the radiocesium penetration in the soil. In order to use this formula, we calculated the  $^{137}\text{Cs}$   
159 inventory using  $^{137}\text{Cs}$  activities ( $\text{Bq.kg}^{-1}$ ) (Lee et al., 2013) at the successive (x) depths (Eq. 2):

160  $I(x) = \rho(x) * h(x) * A(x)$  (2)

161 Where  $\rho$  is the dry bulk density ( $\text{g.m}^{-3}$ ),  $h$  is the thickness (cm) of the layer and  $A$  the activity  
162 ( $\text{Bq.kg}^{-1}$ ) of this layer.

163 **B. Behaviour of  $^{110m}\text{Ag}$  in rivers**

164 *Experiment 3 – Activities in sediment sequences accumulated in reservoirs*

165 During the November 2012 fieldwork campaign, we had the opportunity to collect samples  
166 of the different layers representative of the deep sediment sequence that accumulated  
167 behind Tetsuzen dam on Ota River (1.6 m) and behind Takanokura dam on Mizunashi River  
168 (Nitta catchment) (0.5 m) in order to investigate  $^{110m}\text{Ag}$  behaviour in respectively 9 and 7  
169 different layers (Dam Sed 1 and Dam Sed 2 - Fig. 3). We removed the exposed sediment  
170 lateral surface to avoid artificial sample contamination during fieldwork.

171 Particle size of the samples was measured using a SALD-3100 Laser (Shimadzu Co., Ltd.,  
172 Kyoto, Japan) following standard procedures. The particles were classified into 42 size ranges  
173 between 0.05 and 450  $\mu\text{m}$ . The surface specific area was estimated using the density of  
174 quartz ( $2.65\text{g cm}^{-3}$ ) and assuming that particles were spherical (Santamarina and Klein,  
175 2002). Grain size distribution was corrected using sieving data for classes  $>450\mu\text{m}$ , and final  
176 classes were reclassified according to the grain-size ranges proposed by AFNOR X 316107  
177 (i.e., clay  $<2\mu\text{m}$ , 2  $\mu\text{m} <$  silt  $< 50\mu\text{m}$ , 50  $\mu\text{m} <$  sand  $< 2\text{mm}$ ).

178     *Experiment 4 – Impact of typhoon and snowmelt on activities in river drape sediment*

179     A last experiment was conducted in upper parts of the Nitta River catchment (with  
180     elevation > 400m), where the  $^{110m}\text{Ag} : ^{137}\text{Cs}$  activity ratio in soils is low but overall radioactive  
181     contamination is high. This area was impacted by summer typhoons and spring snowmelt  
182     events that generated soil erosion on hillslopes and led to an increase in river discharge  
183     (Fukuyama et al., 2005; Iida et al., 2012; Ueda et al., 2013). Sediment drape deposits (SDD)  
184     were selected as an alternative to suspended sediment in order to increase the spatial  
185     coverage of the survey within the catchments, and to avoid the logistical problems  
186     associated with the collection of suspended sediment in rivers. Olley et al. (2013)  
187     demonstrated that sediment source apportionment conducted on SDD and suspended  
188     matters showed similar results. To prepare a representative sample, five to ten subsamples  
189     that are likely to have deposited after the last major flood were collected at several locations  
190     selected randomly down to the underlying coarser cobble or gravel layer across a 10m<sup>2</sup>  
191     surface. Sediment drape deposits are likely to integrate deposits of the last hydro-  
192     sedimentary events of low to intermediate magnitude (Evrard et al., 2011) even though the  
193     occurrence of large floods probably leads to a complete flush of the system justifying the  
194     relevance of conducting field surveys to collect sediment drape deposits as frequently as  
195     possible.

196     Activities were measured in 4 representative SDD samples collected at the same location  
197     during the four successive fieldwork campaigns (SDD 1 to SDD 4 - Fig. 3). Grain size  
198     measurements were conducted by following the same protocol as described for Experiment  
199     3.

200        2.3 Gamma spectrometry measurements

201 Before measurement, samples were dried at 40°C (105°C for soil), ground to a fine powder  
202 and then packed into 15mL polyethylene specimen cups. Radionuclide activities ( $^{134}\text{Cs}$ ,  $^{137}\text{Cs}$ ,  
203  $^{110\text{m}}\text{Ag}$ ) in all samples were determined by gamma spectrometry using very low-background  
204 coaxial N- and P-types HPGe detectors (Canberra / Ortec). Counting times of soil and  
205 sediment samples varied between  $8\times 10^4$  and  $200\times 10^4$  s to allow the detection of  $^{110\text{m}}\text{Ag}$ ,  
206 which was present in much lower activities in the samples (2–2400 Bq.kg $^{-1}$ ) than  $^{134}\text{Cs}$  and  
207  $^{137}\text{Cs}$  (500–1,245,000 Bq.kg $^{-1}$ ).

208 The  $^{137}\text{Cs}$  activities were measured at the 661 keV emission peak. The  $^{134}\text{Cs}$  ( $T_{1/2} = 2\text{y}$ )  
209 activities were calculated as the mean of activities derived from measurements conducted at  
210 604 keV and 795 keV ( $^{228}\text{Ac}$  activities being negligible compared to  $^{134}\text{Cs}$  activities) as both  
211 peaks are associated with the largest gamma emission intensities of this radionuclide.

212 The presence of  $^{110\text{m}}\text{Ag}$  was confirmed by the detection of an emission peak at 885 keV (as  
213 the peak associated with the largest emission intensity at 658 keV was masked by the 661-  
214 keV peak of  $^{137}\text{Cs}$ ). Minimum detectable activities in  $^{110\text{m}}\text{Ag}$  for 24h counting times reached 2  
215 Bq.kg $^{-1}$ . Detection of  $^{110\text{m}}\text{Ag}$  was considered relevant when the 885 keV peak was present.  
216 Because of their low level, activities in  $^{110\text{m}}\text{Ag}$  were associated with larger uncertainties than  
217 activities in  $^{137}\text{Cs}$ . Counting efficiencies and quality assurance were conducted using internal  
218 and certified International Atomic Energy Agency (IAEA) reference materials prepared in the  
219 same specimen cups as the samples. Uncertainties on results were estimated by combining  
220 counting statistics and calibration uncertainties. Summing and self-absorption effects were  
221 taken into account by analysing standards with similar densities and characteristics as the  
222 collected samples. All radionuclide activities were decay corrected to the date of 14 March  
223 2011 corresponding to the date of the first radionuclide deposits on soils. Most of them

224 were estimated to have deposited on 15 March in Fukushima Prefecture (Kinoshita et al.,  
225 2011; Shozugawa et al., 2012).

226 **3. Results and discussion**

227 **A. Behaviour of  $^{110m}\text{Ag}$  in soils**

228 **Experiment 1 – Affinity with different grain size fractions (Soil 1 to Soil 4)**

229 During this experiment,  $^{110m}\text{Ag}$  activities could only be detected in all fractions for 2 of the 4  
230 analysed samples (Soil 1 and Soil 2 – Fig. 3) as a result of low  $T_{1/2}$  and low  $^{110m}\text{Ag}$  initial  
231 deposition level. Samples were indeed collected in the vicinity of the main contamination  
232 plume as access to the most affected area was restricted by Japanese authorities. It also has  
233 been detected in the finest fraction of the Soil 4 sample. Fig. 4 describes the distribution of  
234  $^{110m}\text{Ag}$  and  $^{137}\text{Cs}$  radionuclides in the different grain size fractions of Soil 1 and Soil 2 samples.

235 Activity distribution is similar for both radionuclides and the major part (from 33% to 65%) of  
236 their activity was measured in the finest fraction ( $<63\mu\text{m}$ ; Table 3). We could therefore not  
237 detect any difference in the particle-size effects of adsorption between both radionuclides.

238 This finding is crucial in order to use the  $^{110m}\text{Ag} : ^{137}\text{Cs}$  activity ratio to track the dispersion of  
239 contaminated particles in catchments, as the finest particles are the most susceptible to be  
240 eroded and redistributed (Motha et al., 2002).

241 **Experiment 2 – Migration in soil (Profile)**

242 Activities measured in the uppermost part of the soil profile (Fig. 3) confirmed the low  
243 mobility of  $^{134}\text{Cs}$ ,  $^{137}\text{Cs}$  and  $^{110m}\text{Ag}$  (Table 4). The bulk of their inventories ( $\approx 80\%$ ) were  
244 contained in the first layers (0 – 8 mm) and decreased rapidly with depth (Fig. 5).

245 The  $^{137}\text{Cs}$  total inventory reached about  $417 \text{ kBq.m}^{-2}$  and the relaxation mass depth  $h_0$  was  
246  $7.1\text{kg.m}^{-2}$  for  $^{137}\text{Cs}$  (Fig. 6). This value is close to the one found by Kato et al. (2012b) in a  
247 cultivated soil ( $9.1 \text{ kg.m}^{-2}$ ) in the vicinity of our sampling site. This value also remained in the  
248 same order of magnitude as in several cultivated soils investigated by Ivanov (Ivanov et al.,  
249 1997) near the Chernobyl Power Plant (ranging from  $5.6$  to  $9.1 \text{ kg.m}^{-2}$ ).

250 In order to compare the behaviour of both radionuclides, we calculated in the same way the  
251 relaxation mass depth for the  $^{110m}\text{Ag}$  and found  $7.6 \text{ kg.m}^{-2}$  with a total  $^{110m}\text{Ag}$  inventory value  
252 of  $1 \text{ kBq.m}^{-2}$ , showing that penetration of both radionuclides in the soil was similar.

253 Our results are consistent with the ones provided by other studies that investigated the  
254 behaviour of the same radionuclides in soils. Alloway (1995) showed that  $^{110m}\text{Ag}$  is not  
255 mobile as it is the case for  $^{137}\text{Cs}$  (Sawi-iney, 1972; Spezzano, 2005) and they both remain in  
256 the uppermost 5cm of the soil (Handl et al., 2000; Kato et al., 2012b; Shang and Leung, 2003)

257 We investigated the migration of radionuclides in a profile of bare soil, but the transposition  
258 of those results to soils covered with vegetation is not straightforward, as the radionuclide  
259 interception and migration processes were reported to play a major role in forested  
260 environments (Kato et al., 2012a). Furthermore, Martin et al. (1989) reported that during the  
261 first months that followed Chernobyl fallout,  $^{110m}\text{Ag}$  required more time to migrate from  
262 grass to soil (50% reduction) than  $^{137}\text{Cs}$  (90% reduction) due to foliar leaching. However, this  
263 effect should have remained limited in Fukushima, as most cultivated soils (i.e., paddy fields)  
264 were found to be bare when atmospheric fallout occurred in March 2011.

265 These results confirm the low mobility of  $^{110m}\text{Ag}$  in cultivated soils. As it remained  
266 concentrated in the first layers, it could be rapidly redistributed across hillslopes as a  
267 consequence of runoff and soil erosion.

268       **C. Behaviour of  $^{110m}\text{Ag}$  in rivers**

269       **Experiment 3 – Activities in sediment sequences accumulated in reservoirs (Dam Sed 1 & 2)**

270 The pH measured in the four investigated rivers varied between 5.0 and 6.0. It was  
271 demonstrated in the literature that pH plays a major role on  $^{110m}\text{Ag}$  behaviour in both soil  
272 and water. Its mobility in soils (Khan et al., 1982; Shang and Leung, 2003) increases when pH  
273 raises and its affinity for suspended particulate matter (SPM) rises when pH exceeds 7, to  
274 reach maximum values at a pH of 9 (Fukai and Murray, 1974; Murray and Murray, 1972). In  
275 contrast,  $^{137}\text{Cs}$  was shown not to be affected by a pH variation (Adam et al., 2001). Because  
276 the observed pH values remained significantly lower than 7,  $^{110m}\text{Ag}$  behaviour and  
277  $^{110m}\text{Ag}$ : $^{137}\text{Cs}$  activity ratio were not expected to be affected by pH variations in Fukushima  
278 rivers.

279 Analysis of the two sediment profiles (Dam Sed 1 and 2 – Fig. 3) tends to confirm the similar  
280 post-depositional behaviour of the radionuclides (Figs. 7 and 8). Their activities were  
281 concentrated in the top of the profile (Tables 5 and 6), and most likely resulted from  
282 deposition of sediment eroded after the initial radionuclide fallout in March 2011. Before  
283 the FDNPP accident,  $^{137}\text{Cs}$  activities in sediment were generally lower than 100Bq/kg in  
284 Japanese soils (Fukuyama et al., 2005), which corresponds to activities found in deeper  
285 layers of sediment accumulated behind Tetsuzen dam (Dam Sed 1). Higher contamination in  
286 lower layers in the second profile ( $> 500\text{Bq/kg}$ ) most likely resulted from contamination

287 originating from upper levels during sampling (scraping). However, this will not impact the  
288 conclusions drawn from this experiment as they strictly focus on the observations made on  
289 the top layers.

290 In Tetsuzen dam sediment (Dam Sed 1), a lower activity was measured in the surface layer  
291 than in the underlying layer suggesting that a minimum of two significant erosion events had  
292 supplied contaminated sediment to the reservoir by November 2012 (Fig. 7; Table 5). Also,  
293  $^{110m}\text{Ag}/^{137}\text{Cs}$  activity ratio remained constant for these layers. Furthermore, a significant  
294 difference in particle size between the first two layers and the third layer confirms the  
295 occurrence of an intense erosion event, probably during the dam release that was carried  
296 out during the period of heavy typhoons that took place during summer in 2011. Based on  
297 this information, sedimentation rates were estimated to  $20\text{cm yr}^{-1}$  in Tetsuzen dam, and to  
298  $5\text{cm yr}^{-1}$  in Takanokura dam.

299

300 The similar percentage of radionuclide inventories found in the successive layers and the  
301 calculation of constant  $^{110m}\text{Ag}/^{137}\text{Cs}$  activity ratios confirmed that  $^{110m}\text{Ag}$  and  $^{137}\text{Cs}$  have a  
302 similar behaviour with regard to their adsorption onto soil particles and sediment. This result  
303 was expected owing to the high distribution coefficients reported in the literature for both  
304 Cs and Ag (Ciffroy et al., 2001; Fournier-Bidoz and Garnier-Laplace, 1994).  $K_d$  values  
305 remaining in the same order of magnitude were estimated for both radionuclides in winter  
306 and summer (i.e.  $K_{d\text{Cs}}^{^{137}}$  : 0.1-100;  $K_{d\text{Ag}}^{^{110m}}$  : 1-100). Ciffroy et al. (2001) also quantified the  
307 kinetics of the adsorption and desorption of these radionuclides in freshwater systems, and  
308 concluded to their similar behaviour. Fournier-Bidoz and Garnier-Laplace (1994) and Garnier  
309 et al. (2006) showed that  $^{110m}\text{Ag}$  has a strong affinity for river SPM and especially for their

310 clay fraction. A large number of studies demonstrated that Cs has the same behaviour  
311 (Ojima et al. , 1965 in Ancelin et al., 1979; Garnier-Laplace et al., 1994). He and Walling  
312 (1996) confirmed that  $^{137}\text{Cs}$  affinity increases with specific surface area in the case of a  
313 uniform contamination of the soils. Guégueniat et al. (1976) reported similar results for  
314  $^{110\text{m}}\text{Ag}$ .

315 **Experiment 4 – Impact of typhoon and snowmelt**

316 During the three successive sampling campaigns that followed the succession of snowmelt  
317 and typhoon events, the inventories of  $^{110\text{m}}\text{Ag}$  and  $^{137}\text{Cs}$  measured in sediment drape  
318 deposits collected systematically at four sampling points in the upper part of the Nitta  
319 catchment (Fig. 3) showed similar patterns (Fig. 9). As expected, samples collected close to  
320 the catchment headwaters (SDD 1 and SDD 4) showed a decrease in contamination  
321 throughout time, probably due to the flush of the most contaminated material during high  
322 water flows (Table 7). In contrast, the samples collected at the 2 downstream locations  
323 (especially SDD 3) were associated with a slight temporal increase in contamination of  $^{137}\text{Cs}$   
324 that may be explained by a supply of upstream – more contaminated – material. This  
325 explanation is consistent with the fact that  $^{110\text{m}}\text{Ag}:\text{:}^{137}\text{Cs}$  activity ratio measured in sediment  
326 remained in the same order of magnitude as the ratio measured in soils of this upper part of  
327 the Nitta catchment (Table 8).

328 An alternative explanation to the activity increase observed throughout time is that the grain  
329 size of particles could have changed from one campaign to the next, explaining the observed  
330 differences in contamination. Calculation of surface specific area (SSA) shown in Fig. 9 shows  
331 that this might be the case for sample SDD 3 (with an enrichment in fine particles  
332 throughout time), but not for sample SDD 2 (SSA remaining constant in time).

333 Because of different experimental conditions (non-homogeneous fallout deposition and high  
334 radionuclide activities), our results plotted on Fig. 10 do not show a power function as found  
335 by He and Walling (1996) but they display instead a linear function for both  $^{137}\text{Cs}$  ( $r^2 = 0.89$ )  
336 and  $^{110\text{m}}\text{Ag}$  ( $r^2 = 0.91$ ) that is strongly correlated with the SSA.

337 This tends to confirm the similar behaviour for both radionuclides, although particle-size  
338 effects and fractionation could have occurred, given that erosion and transport in rivers are  
339 obviously selective to finer particles. Consequently, these results confirmed the relevance of  
340 using of  $^{110\text{m}}\text{Ag}:\text{ }^{137}\text{Cs}$  activity ratio to investigate the dispersion and redistribution of  
341 contamination along rivers.

342 **Conclusions**

343 Silver-110m ( $^{110\text{m}}\text{Ag}$ ) is an anthropogenic radionuclide that is produced continuously by  
344 nuclear power plants (NPP) in normal conditions, but investigations regarding its behaviour  
345 in the environment are rare despite the potentially important radioecological implications of  
346 its accidental release into the environment. In the Fukushima NPP post-accidental context,  
347 the interest to conduct field studies on the behaviour of  $^{110\text{m}}\text{Ag}$  was reinforced by the fact  
348 that initial deposits displayed  $^{110\text{m}}\text{Ag}:\text{ }^{137}\text{Cs}$  activity ratios that varied across space within the  
349 main radioactive contamination plume. This study showed that  $^{137}\text{Cs}$  and  $^{110\text{m}}\text{Ag}$  were  
350 strongly sorbed by the finest particle fractions (i.e., clay or silt), and that the bulk of their  
351 inventory was stored in the uppermost part of soil profiles (i.e., <2 cm), confirming that the  
352 in-depth mobility was not significant during the two years following the accident. In addition  
353 to this fine particle reactivity, we showed that soil erosion and sediment transport in  
354 catchments that mobilize preferentially the finest particle fractions did not induce different  
355 fractionation effects for both radionuclides. This study therefore confirmed the relevance of

356 using this ratio to track the dispersion of contaminated material along coastal rivers draining  
357 this area. In future, due to the rapid decay of radiosilver and its initially relatively low fallout  
358 level, extraction methods could be used in order to measure precisely radiosilver and  
359 continue to investigate its behaviour and the dispersion of contaminated sediment along  
360 rivers.

361 **Acknowledgements**

362 This work was a part of the TOFU (Tracing the environmental consequences of the Tohoku  
363 earthquake-triggered tsunami and Fukushima accident) project, funded by the joint French  
364 National Research Agency-Flash Japon (ANR- 11-JAPN-001) and Japan Science and  
365 Technology agency/J-RAPID programme. H. L. received a PhD fellowship from CEA  
366 (Commissariat à l'Energie Atomique et aux Energies Alternatives).

367

368

369    **References**

- 370    Adam, C., Baudin, J.P., Garnier-laplace, J., 2001. Kinetics of Ag-110m, Co-60, Cs-137 and Mn-  
371        54 bioaccumulation from water and depuration by the Crustacean Daphnia magna.  
372        Water Air Soil Pollut. 125, 171–188.
- 373    Ancelin, J., Guéguéniat, P., Germain, P., 1979. Radioécologie marine, étude du devenir des  
374        radionucléides rejetés en milieu marin et application à la radioprotection, Eyrolles. ed.  
375        Paris.
- 376    Beresford, N.A., Crout, N.M.J., Mayes, R.W., Howard, B.J., Lamb, C.S., 1998. Dynamic  
377        distribution of radioisotopes of cerium, ruthenium and silver in sheep tissues. J.  
378        Environ. Radioact. 38, 317–338.
- 379    Bryan, G.W., 1971. Effects of heavy metals (other than Mercury) on marine and estuarine  
380        organisms. Proc. R. Soc. Ser. B - Biol. Sci. 177, 389.
- 381    Bryan, G.W., Langston, W.J., 1992. Bioavailability, accumulation and effects of heavy metals  
382        in sediments with special reference to United Kingdom estuaries: a review. Environ.  
383        Pollut. 76, 89–131.
- 384    Buesseler, K.O., Jayne, S.R., Fisher, N.S., Rypina, I.I., Baumann, H., Baumann, Z., Breier, C.F.,  
385        Douglas, E.M., George, J., Macdonald, A.M., Miyamoto, H., Nishikawa, J., Pike, S.M.,  
386        Yoshida, S., 2012. Fukushima-derived radionuclides in the ocean and biota off Japan.  
387        Proc. Natl. Acad. Sci. U. S. A. 5984-5988, 1–7.
- 388    Calmon, P., Garnier-Laplace, J., 2002. Fiche radionucléide - Argent-110m et environnement.  
389        IRSN 15.

- 390 Chartin, C., Evrard, O., Onda, Y., Patin, J., Lefèvre, I., Ottlé, C., Ayrault, S., Lepage, H., Bonté,  
391 P., 2013. Tracking the early dispersion of contaminated sediment along rivers draining  
392 the Fukushima radioactive pollution plume. *Anthropocene* 1, 23–34.
- 393 Chelet, Y., 2006. La radioactivité - Manuel d'initiation, Nucléon. ed.
- 394 Chino, M., Nakayama, H., Nagai, H., Terada, H., Katata, G., Yamazawa, H., 2011. Preliminary  
395 Estimation of Release Amounts of  $^{131}\text{I}$  and  $^{137}\text{Cs}$  Accidentally Discharged from the  
396 Fukushima Daiichi Nuclear Power Plant into the Atmosphere. *J. Nucl. Sci. Technol.* 48,  
397 1129–1134.
- 398 Ciffroy, P., Garnier, J.-M., Pham, M.K., 2001. Kinetics of the adsorption and desorption of  
399 radionuclides of Co, Mn, Cs, Fe, Ag and Cd in freshwater systems: experimental and  
400 modelling approaches. *J. Environ. Radioact.* 55, 71–91.
- 401 Ciffroy, P., Siclet, F., Damois, C., Luck, M., Duboudin, C., 2005. A dynamic model for assessing  
402 radiological consequences of routine releases in the Loire river: parameterisation and  
403 uncertainty/sensitivity analysis. *J. Environ. Radioact.* 83, 9–48.
- 404 Evrard, O., Navratil, O., Ayrault, S., Ahmadi, M., Némery, J., Legout, C., Lefèvre, I., Poirel, A.,  
405 Bonté, P., Esteves, M., 2011. Combining suspended sediment monitoring and  
406 fingerprinting to determine the spatial origin of fine sediment in a mountainous river  
407 catchment. *Earth Surf. Process. Landforms* 36, 1072–1089.
- 408 Evrard, O., Chartin, C., Onda, Y., Patin, J., Lepage, H., Lefèvre, I., Ayrault, S., Ottlé, C., Bonté,  
409 P. (2013). Evolution of radioactive dose rates in fresh sediment deposits along rivers  
410 draining Fukushima contamination plume. *Scientific Reports* 3, 3079.

- 411 Eyrolle, F., Radakovitch, O., Rimbault, P., Charmasson, S., Antonelli, C., Ferrand, E., Aubert,  
412 D., Raccasi, G., Jacquet, S., Gurriaran, R., 2012. Consequences of hydrological events on  
413 the delivery of suspended sediment and associated radionuclides from the Rhône River  
414 to the Mediterranean Sea. *J. Soils Sediments* 12, 1479–1495.
- 415 Fournier-Bidoz, V., Garnier-laplace, J., 1994. Etude bibliographique sur les échanges entre  
416 l'eau les matières en suspension et les sédiments des principaux radionucléides rejetés  
417 par les centrales nucléaires, *Radioprotection*. IPSN.
- 418 Fournier-Bidoz, V., Garnier-laplace, J., Baudin, J., 1997. État des connaissances sur les  
419 échanges entre l'eau, les matières en suspension et les sédiments des principaux  
420 radionucléides rejetés par les centrales nucléaires en eau douce. *Radioprotection* 3, 49–  
421 71.
- 422 Fukai, R., Murray, C., 1974. Environmental behavior of radiocobalt and radiosilver released  
423 from nuclear power stations into aquatic systems. *Radioact. Sea* 40, 217–242.
- 424 Fukuda, T., Kino, Y., Abe, Y., Yamashiro, H., Kuwahara, Y., Nihei, H., Sano, Y., Irisawa, A.,  
425 Shimura, T., Fukumoto, Motoi, Shinoda, H., Obata, Y., Saigusa, S., Sekine, T., Isogai, E.,  
426 Fukumoto, Manabu, 2013. Distribution of artificial radionuclides in abandoned cattle in  
427 the evacuation zone of the Fukushima Daiichi nuclear power plant. *PLoS One* 8, e54312.
- 428 Fukuyama, T., Takenaka, C., Onda, Y., 2005.  $^{137}\text{Cs}$  loss via soil erosion from a mountainous  
429 headwater catchment in central Japan. *Sci. Total Environ.* 350, 238–47.

- 430 Garnier, J.-M., Ciffroy, P., Benyahya, L., 2006. Implications of short and long term (30 days)  
431 sorption on the desorption kinetic of trace metals (Cd, Zn, Co, Mn, Fe, Ag, Cs) associated  
432 with river suspended matter. *Sci. Total Environ.* 366, 350–60.
- 433 Guégueniat, P., Gandon, R., Hémon, G., Philippot, J.C., 1976. Méthode de mesure d'éléments  
434 traces dans l'eau de mer par activation neutronique. Cas particulier des isotopes  
435 stables de produits de fission. *Meas. Detect. Control Environ. Pollut.* IAEA-SM, 206/28.
- 436 Handl, J., Kallweit, E., Henning, M., Szwec, L., 2000. On the long-term behaviour of  $^{110}\text{mAg}$   
437 in the soil–plant system and its transfer from feed to pig. *J. Environ. Radioact.* 48, 159–  
438 170.
- 439 He, Q., Walling, D., 1996. Interpreting particle size effects in the adsorption of  $^{137}\text{Cs}$  and  
440 unsupported  $^{210}\text{Pb}$  by mineral soils and sediments. *J. Environ. Radioact.* 30, 117–137.
- 441 IAEA, 1998. Radiological characterization of shut down nuclear reactors for decommissioning  
442 purposes. IAEA, Vienna, Tech. Rep 389, 184.
- 443 Iida, T., Kajihara, A., Okubo, H., Okajima, K., 2012. Effect of seasonal snow cover on  
444 suspended sediment runoff in a mountainous catchment. *J. Hydrol.* 428–429, 116–128.
- 445 Ivanov, Y., Lewyckyj, N., Levchuk, S., 1997. Migration of  $^{137}\text{Cs}$  and  $^{90}\text{Sr}$  from chernobyl  
446 fallout in Ukrainian, Belarussian and Russian soils. *J. Environ. Qual.* 35, 1–21.
- 447 Kato, H., Onda, Y., Gomi, T., 2012a. Interception of the Fukushima reactor accident derived  
448  $^{137}\text{Cs}$ ,  $^{134}\text{Cs}$  and  $^{131}\text{I}$  by coniferous forest canopies. *Geophys. Res. Lett.* 39, L20403.

- 449 Kato, H., Onda, Y., Teramage, M., 2012b. Depth distribution of  $^{137}\text{Cs}$ ,  $^{134}\text{Cs}$ , and  $^{131}\text{I}$  in soil  
450 profile after Fukushima Dai-ichi Nuclear Power Plant Accident. *J. Environ. Radioact.* 111,  
451 59–64.
- 452 Khan, S., Nandan, D., Khan, N.N., 1982. The mobility of some heavy metals through Indian  
453 Red Soil. *Environ. Pollut. Ser. B, Chem. Phys.* 4, 119–125.
- 454 Khangarot, B., Ray, P., 1987. Correlation between heavy metal acute toxicity values  
455 in *Daphnia magna* and fish. *Bull. Environ. Contam. Toxicol.* 38, 722–726.
- 456 Kinoshita, N., Sueki, K., Sasa, K., Kitagawa, J., Ikarashi, S., Nishimura, T., Wong, Y.-S., Satou,  
457 Y., Handa, K., Takahashi, T., Sato, M., Yamagata, T., 2011. Assessment of individual  
458 radionuclide distributions from the Fukushima nuclear accident covering central-east  
459 Japan. *Proc. Natl. Acad. Sci. U. S. A.* 108, 19526–9.
- 460 Koarashi, J., Atarashi-Andoh, M., Matsunaga, T., Sato, T., Nagao, S., Nagai, H., 2012. Factors  
461 affecting vertical distribution of Fukushima accident-derived radiocesium in soil under  
462 different land-use conditions. *Sci. Total Environ. Environ.* 431, 392–401.
- 463 Lee, S.H., Oh, J.S., Lee, J.M., Lee, K.B., Park, T.S., Lujaniene, G., Valiulis, D., Sakalys, J., 2013.  
464 Distribution characteristics of  $(^{137}\text{Cs})$ , Pu isotopes and  $(^{241}\text{Am})$  in soil in Korea. *Appl.*  
465 *Radiat. Isot.* In press.
- 466 Martin, C.J., Heaton, B., Thompson, J., 1989. Cesium-137,  $^{134}\text{Cs}$  and  $^{110}\text{mAg}$  in lambs  
467 grazing pasture in NE Scotland contaminated by Chernobyl fallout. *Health Phys.* 56,  
468 459–64.

- 469 Martin, T.R., Holdich, D.M., 1986. The acute lethal toxicity of heavy metals to peracarid  
470 crustaceans. *Water Res.* 20, 1137–1147.
- 471 Matsunaga, T., Koarashi, J., Atarashi-Andoh, M., Nagao, S., Sato, T., Nagai, H., 2013.  
472 Comparison of the vertical distributions of Fukushima nuclear accident radiocesium in  
473 soil before and after the first rainy season, with physicochemical and mineralogical  
474 interpretations. *Sci. Total Environ. Environ.* 447C, 301–314.
- 475 MEXT, 2011. Preparation of Distribution Map of Radiation Doses ( Map of Tellure 129 and  
476 Silver 110m Concentration in Soil ).
- 477 Murray, C.N., Murray, L., 1972. Adsorption-desorption equilibria of some radionuclides in  
478 sediment-fresh-water and sediment-sea water systems. *Radioact. Contam. Mar.*  
479 *Environ.* 105–122.
- 480 Olley, J., Brooks, A., Spencer, J., Pietsch, T., Borombovits, D., 2013. Subsoil erosion  
481 dominates the supply of fine sediment to rivers draining into Princess Charlotte Bay,  
482 Australia. *J. Environ. Radioact.* 124C, 121–129.
- 483 Oughton, D., 1989. The environmental chemistry of radiocaesium and other nuclides.  
484 University of Manchester.
- 485 Petit, G., Douyset, G., Ducros, G., Gross, P., Achim, P., Monfort, M., Raymond, P., Pontillon,  
486 Y., Jutier, C., Blanchard, X., Taffary, T., Moulin, C., 2012. Analysis of Radionuclide  
487 Releases from the Fukushima Dai-Ichi Nuclear Power Plant Accident Part I. *Pure Appl.*  
488 *Geophys.*

- 489 Ratte, H.T., 1999. Bioaccumulation and toxicity of silver compounds: A review. Environ.  
490 Toxicol. Chem. 18, 89–108.
- 491 Santamarina, J., Klein, K., 2002. Specific surface: determination and relevance. Can. Geotech.  
492 241, 233–241.
- 493 Shang, Z.R., Leung, J.K.C., 2003. 110m Ag root and foliar uptake in vegetables and its  
494 migration in soil. J. Environ. Radioact. 65, 297–307.
- 495 Shozugawa, K., Nogawa, N., Matsuo, M., 2012. Deposition of fission and activation products  
496 after the Fukushima Dai-ichi nuclear power plant accident. Environ. Pollut. 163, 243–7.
- 497 Stohl, A., Seibert, P., Wotawa, G., Arnold, D., Burkhardt, J.F., Eckhardt, S., Tapia, C., Vargas, A.,  
498 Yasunari, T.J., 2012. Xenon-133 and caesium-137 releases into the atmosphere from the  
499 Fukushima Dai-ichi nuclear power plant: determination of the source term, atmospheric  
500 dispersion, and deposition. Atmos. Chem. Phys. 12, 2313–2343.
- 501 Tanaka, K., Sakaguchi, A., Kanai, Y., Tsuruta, H., Shinohara, A., Takahashi, Y., 2012.  
502 Heterogeneous distribution of radiocesium in aerosols, soil and particulate matters  
503 emitted by the Fukushima Daiichi Nuclear Power Plant accident: retention of micro-  
504 scale heterogeneity during the migration of radiocesium from the air into ground and  
505 rive. J. Radioanal. Nucl. Chem. 295, 1927–1937.
- 506 Tateda, Y., Tsumune, D., Tsubono, T., 2013. Simulation of radioactive cesium transfer in the  
507 southern Fukushima coastal biota using a dynamic food chain transfer model. J.  
508 Environ. Radioact. 124, 1–12.

- 509 Tazoe, H., Hosoda, M., Sorimachi, A., Nakata, A., Yoshida, M. a, Tokonami, S., Yamada, M.,  
510 2012. Radioactive pollution from Fukushima Daiichi nuclear power plant in the  
511 terrestrial environment. *Radiat. Prot. Dosimetry* 152, 198–203.
- 512 Ueda, S., Hasegawa, H., Kakiuchi, H., Akata, N., Ohtsuka, Y., Hisamatsu, S., 2013. Fluvial  
513 discharges of radiocaesium from watersheds contaminated by the Fukushima Dai-ichi  
514 Nuclear Power Plant accident, Japan. *J. Environ. Radioact.* 118, 96–104.
- 515 Vuković, Ž., 2002. Environmental impact of radioactive silver released from nuclear power  
516 plant. *J. Radioanal. Nucl. Chem.* 254, 637–639.
- 517 Watanabe, T., Tsuchiya, N., Oura, Y., Ebihara, M., 2012. Distribution of artificial radionuclides  
518 (110mAg, 129mTe, 134Cs, 137Cs) in surface soils from Miyagi Prefecture, northeast  
519 Japan, following the 2011 Fukushima Dai-ichi nuclear power. *Geochem. J.* 46, 279–285.
- 520 Winiarek, V., Bocquet, M., Saunier, O., Mathieu, A., 2012. Estimation of errors in the inverse  
521 modeling of accidental release of atmospheric pollutant: Application to the  
522 reconstruction of the cesium-137 and iodine-131 source terms from the Fukushima  
523 Daiichi power plant. *J. Geophys. Res.* 117, 1–16.
- 524 Yasunari, T., Stohl, A., Hayano, R.S., Burkhardt, J.F., Eckhardt, S., 2011. Cesium-137 deposition  
525 and contamination of Japanese soils due to the Fukushima nuclear accident. *Proc. Natl.*  
526 *Acad. Sci. U. S. A.* 108, 19530–4.
- 527
- 528

529 **Figure captions**

530 Figure 1. Number of publications per year between 1937 and 2013 based on a search in the  
531 Web of Knowledge citation index, using “radiosilver” (or “Ag-110m” » or “ $^{110m}\text{Ag}$ ”) and  
532 “environment” as topic keywords (22 July 2013).

533 Figure 2. Location of the main radiocaesium ( $^{134}\text{Cs} + ^{137}\text{Cs}$ ) contamination plume in  
534 Fukushima Prefecture, northeastern Japan (derived from MEXT data decay-corrected to June  
535 2011).

536 Figure 3. Location of the samples collected across the main contamination plume of  
537 Fukushima Prefecture. Background map corresponds to  $^{110m}\text{Ag} : ^{137}\text{Cs}$  activity ratio based on  
538 data measured in Fukushima Prefecture by MEXT in June 2011 (activities decay-corrected to  
539 14 June 2011). SDD: sediment drape deposits, Dam Sed 1: sediment collected in Tetsuzen  
540 dam, Dam Sed 2: sediment collected in Takanokura dam; FDNPP: Fukushima Dai-ichi Nuclear  
541 Power Plant.

542 Figure 4. Percentage of total activity in  $^{110m}\text{Ag}$  and  $^{137}\text{Cs}$  in four particle size classes ( $d =$   
543 diameter) for two soil samples (Soil 1 and Soil 2 - see the location of sampling sites on Figure  
544 3).

545 Figure 5. Radionuclide inventory (%) in successive 2-mm increment layers along a bare soil  
546 profile (Profile - see the location of sampling sites on Figure 3).

547 Figure 6. Distribution of  $^{137}\text{Cs}$  inventory (%) in the bare soil profile as measured by gamma  
548 spectrometry and fitted using Eq. (1), as a function of mass depth ( $\text{kg.m}^{-2}$ ) (Profile - see the  
549 location of sampling sites on Figure 3).

550 Figure 7. Sediment profile accumulated in Yokokawa reservoir on the Ota River (Dam Sed 1  
551 – see the location of sampling sites on Figure 3) – a) Picture of the profile: the limits of the  
552 numbered sampled layers are represented with horizontal lines - b) Anthropogenic  
553 radionuclide inventories (%) in the successive layers of the profile (mm) – c) Grain size  
554 composition of the different layers.

555 Figure 8. Sediment profile accumulated behind Takanokura dam on the Mizunashi River  
556 (Nitta catchment – Dam Sed 2 – see the location of sampling sites on Figure 3) – a) Picture of  
557 the profile: the limits of the numbered sampled layers are represented with horizontal lines -  
558 b) Activity in anthropogenic radionuclides in the successive layers of the profile – c) Grain  
559 size composition of the different layers.

560 Figure 9. Evolution of the  $^{137}\text{Cs}$  and  $^{110\text{m}}\text{Ag}$  contamination inventory (%) and specific surface  
561 area (SSA) ( $\text{m}^2 \cdot \text{g}^{-1}$ ) of sediment drape deposits collected in the upper part of the Nitta River  
562 catchment during the campaigns of Nov 2011, April 2012 and Nov 2012 (SDD 1 to SDD 4 –  
563 see the location of sampling sites on Figure 3).

564 Figure 10. Relationships between  $^{137}\text{Cs}$  and  $^{110\text{m}}\text{Ag}$  activities ( $\text{Bq} \cdot \text{kg}^{-1}$ ) and specific surface  
565 area ( $\text{m}^2 \cdot \text{g}^{-1}$ ) in sediment drape deposits collected in the upper part of the Nitta River  
566 catchment during the campaigns of Nov 2011, April 2012 and Nov 2012 (SDD 1 to SDD 4 –  
567 see the location of sampling sites on Figure 3).

Figure 1.

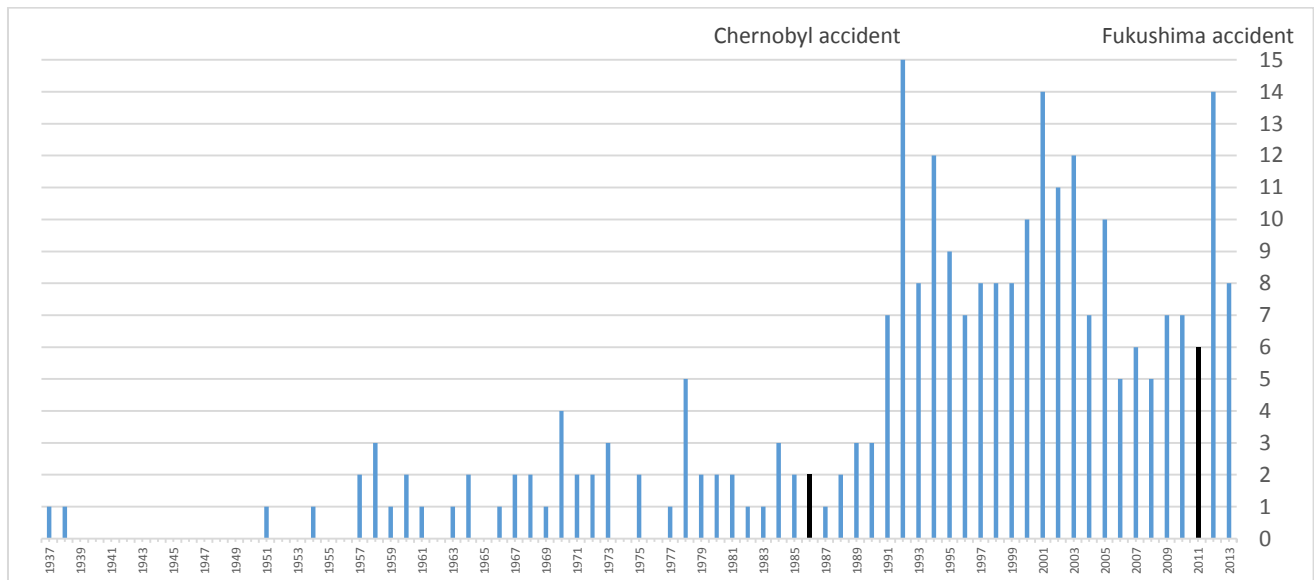


Figure 2.

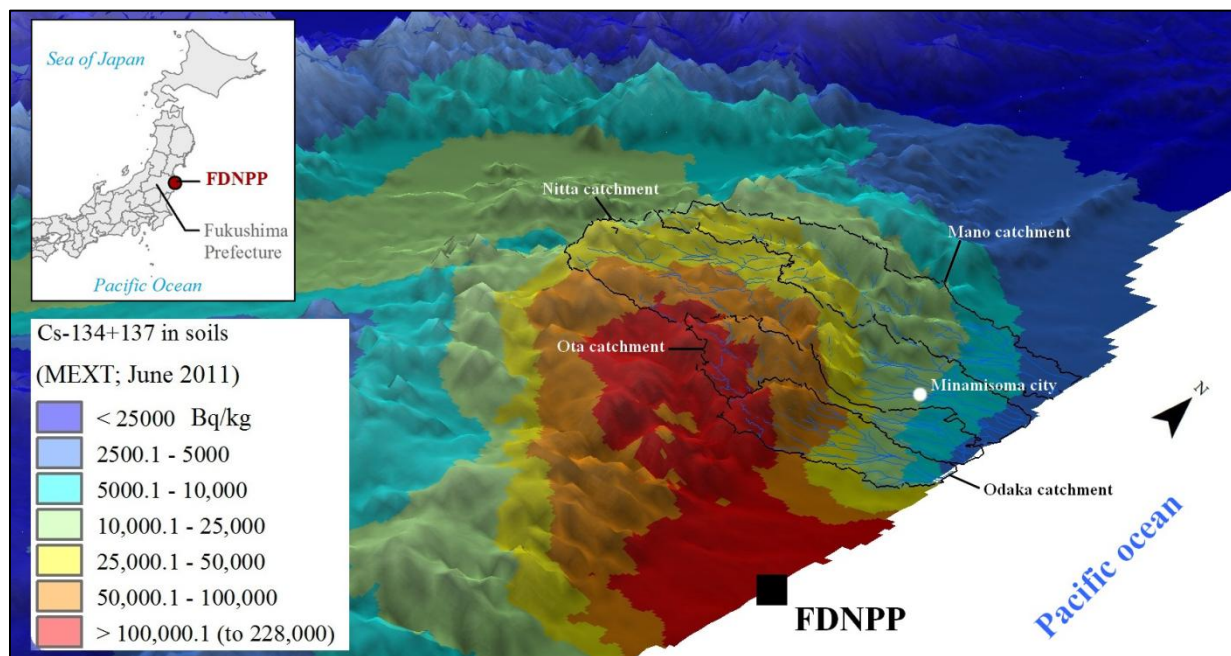


Figure 3.

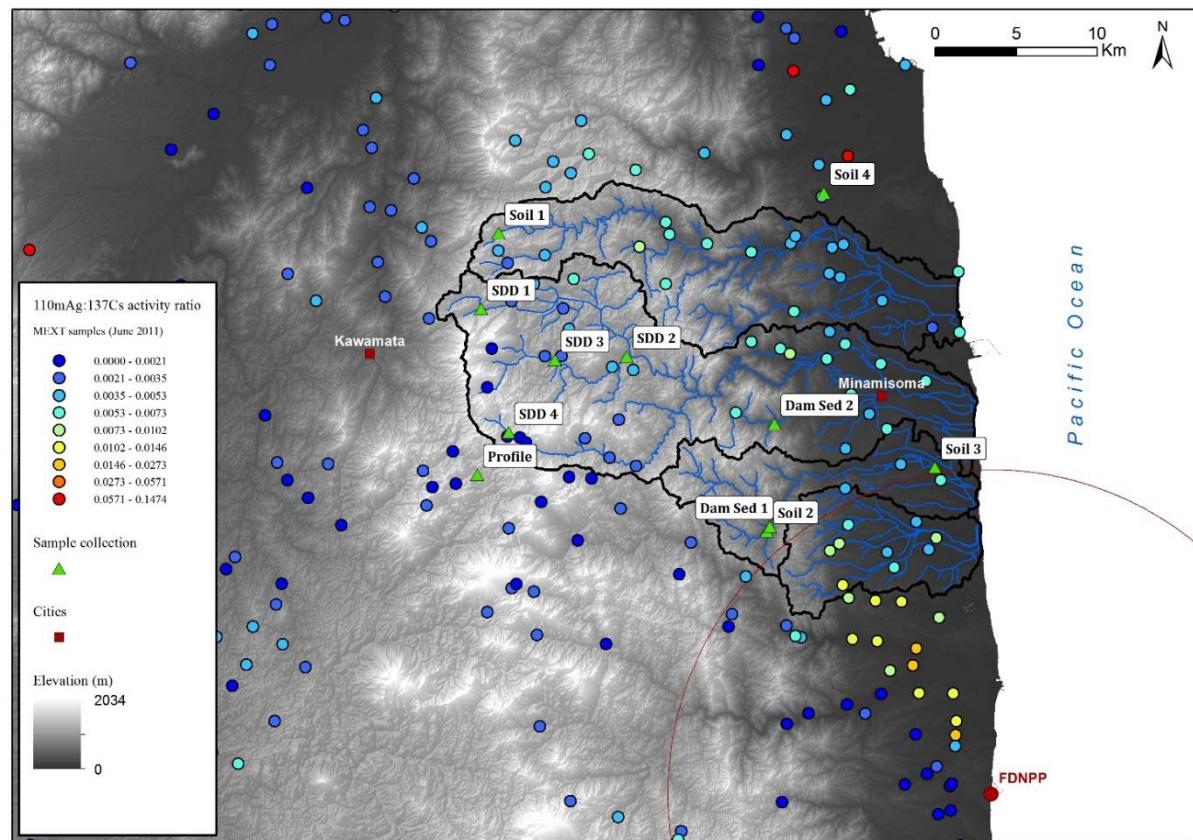


Figure 4.

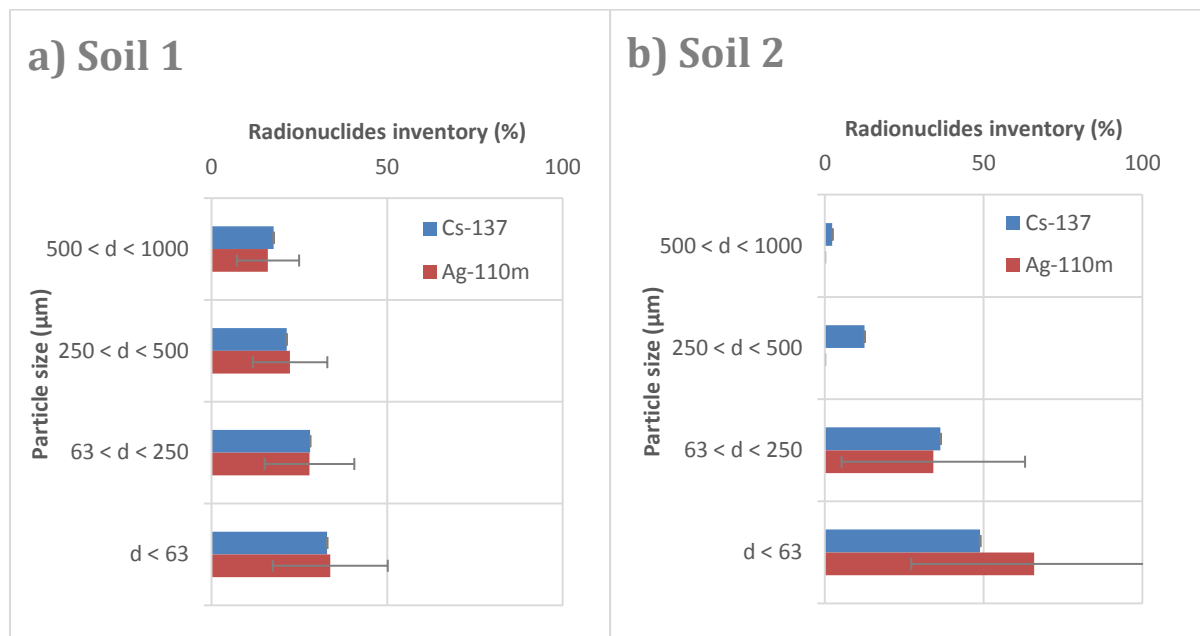


Figure 5.

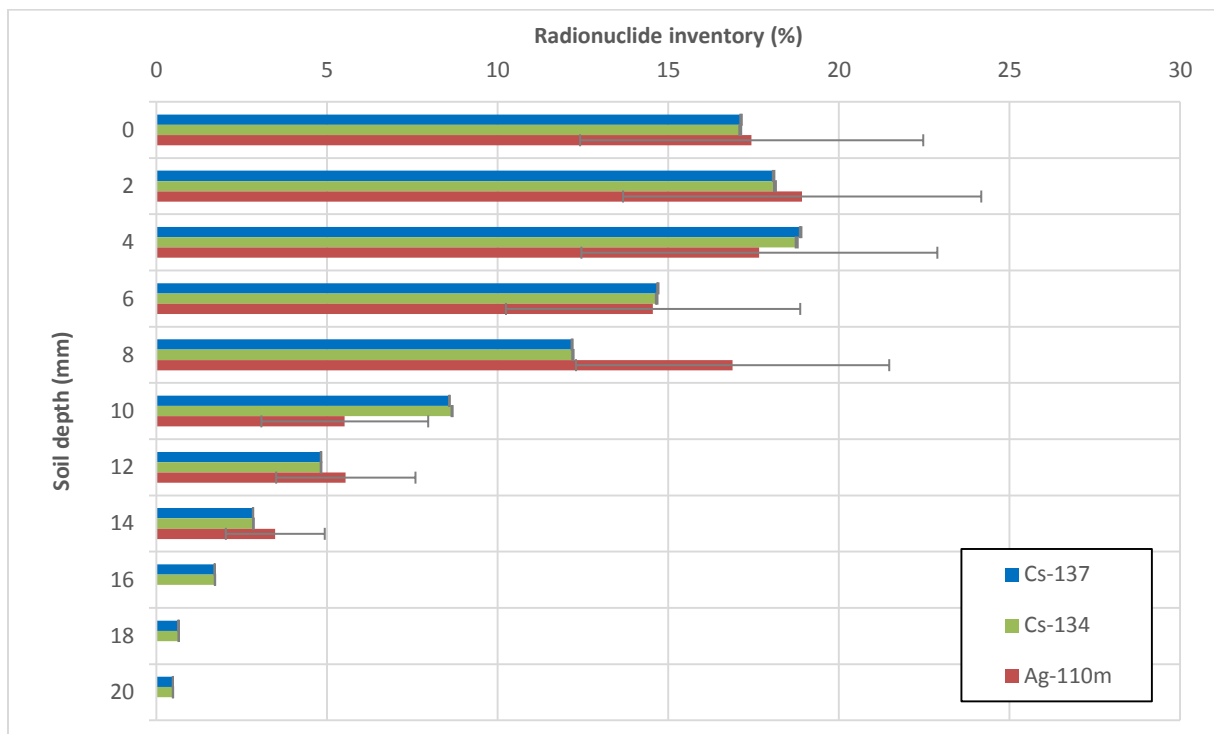


Figure 6.

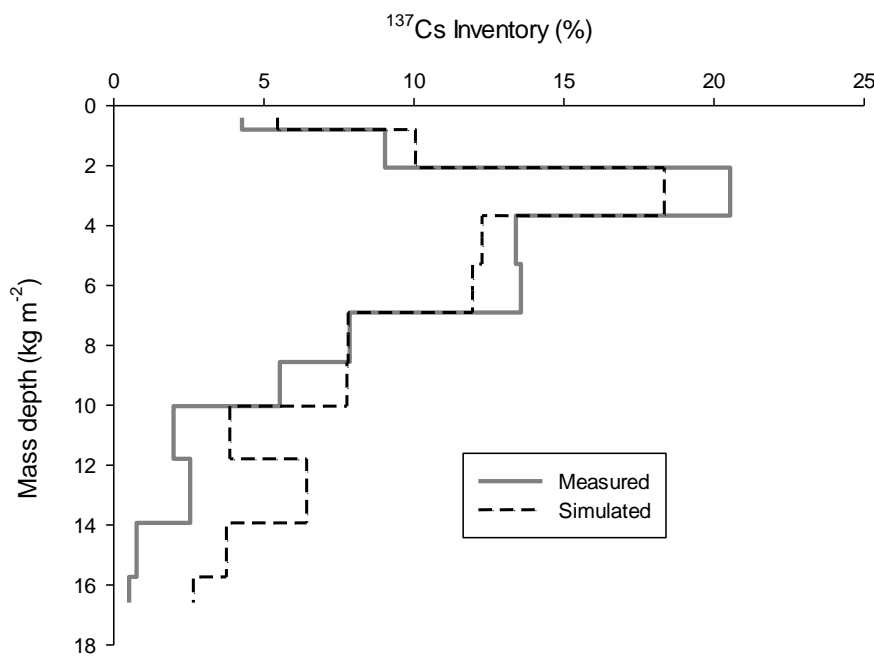


Figure 7.

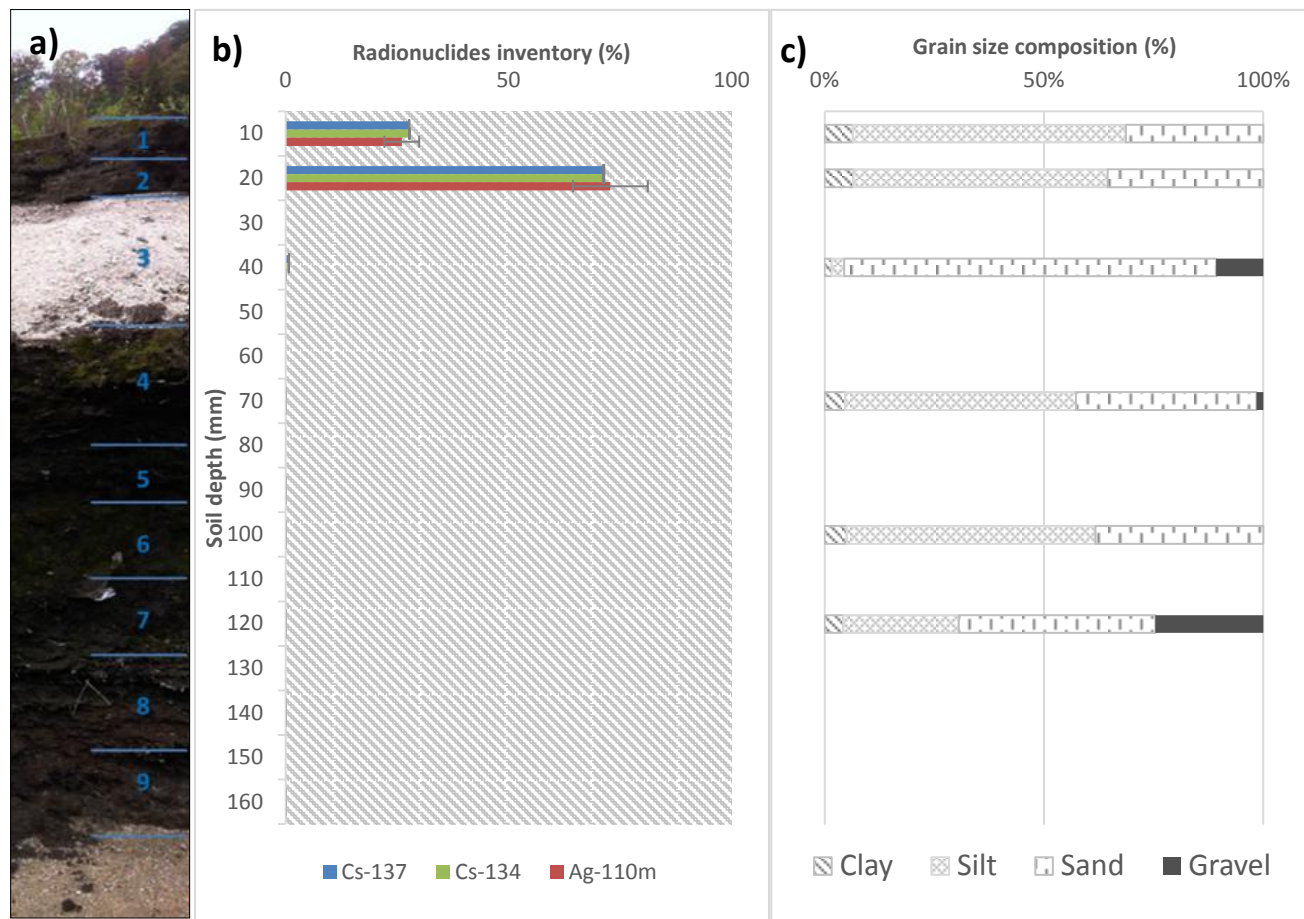


Figure 8.

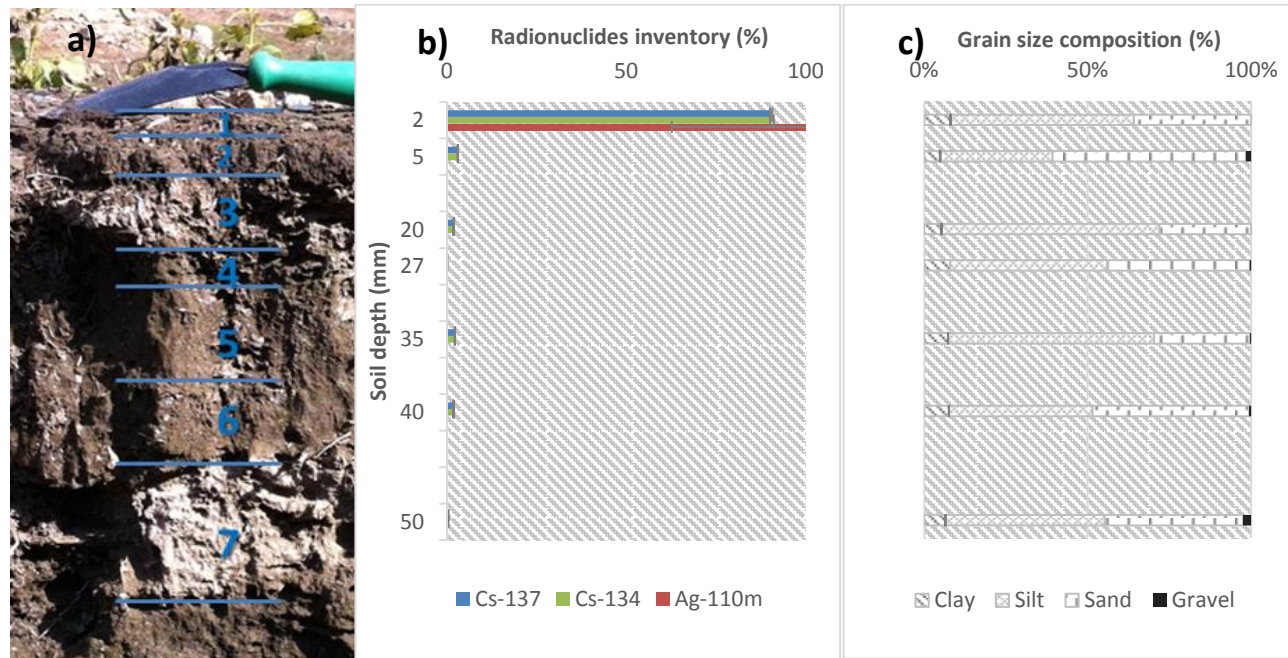


Figure 9.

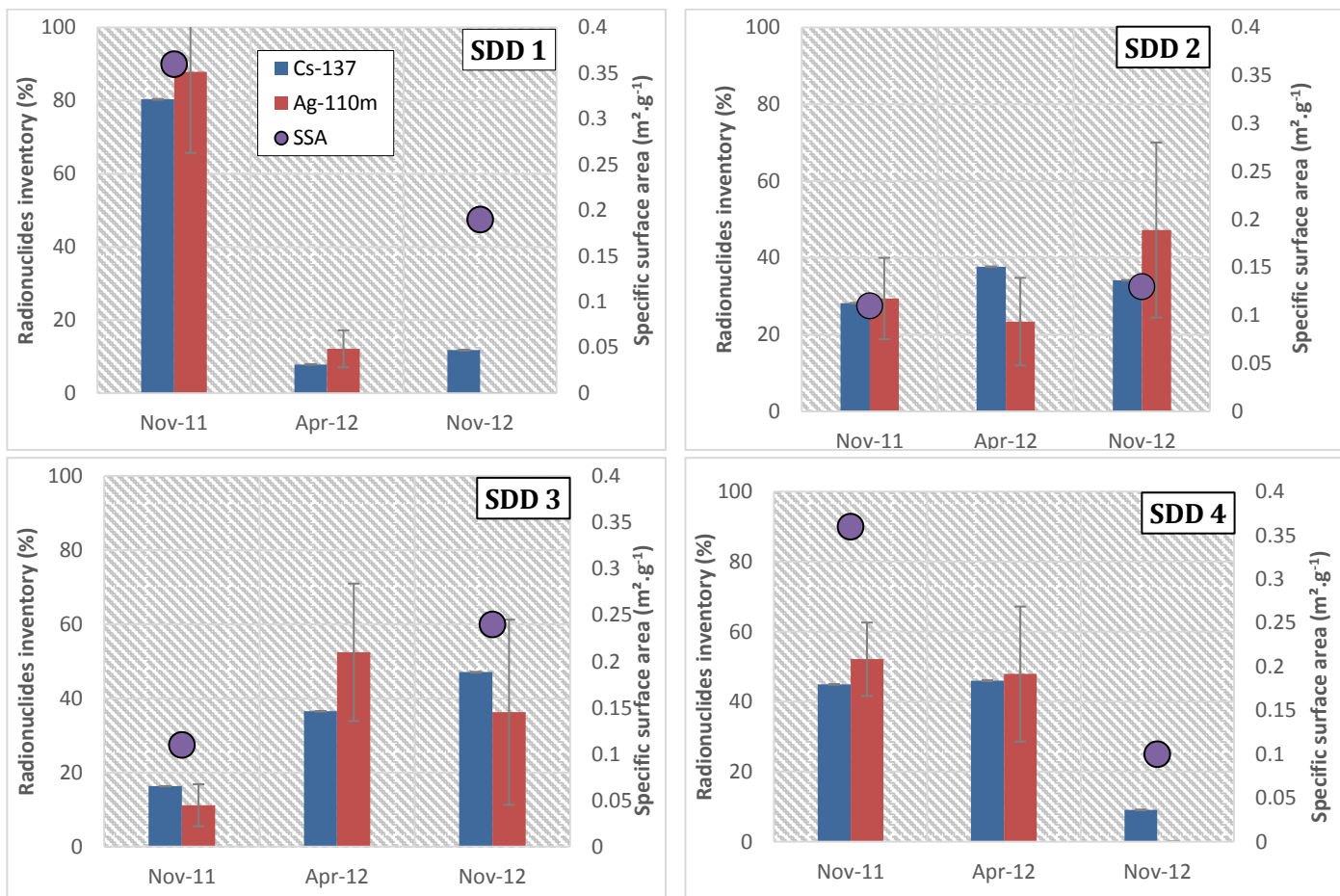
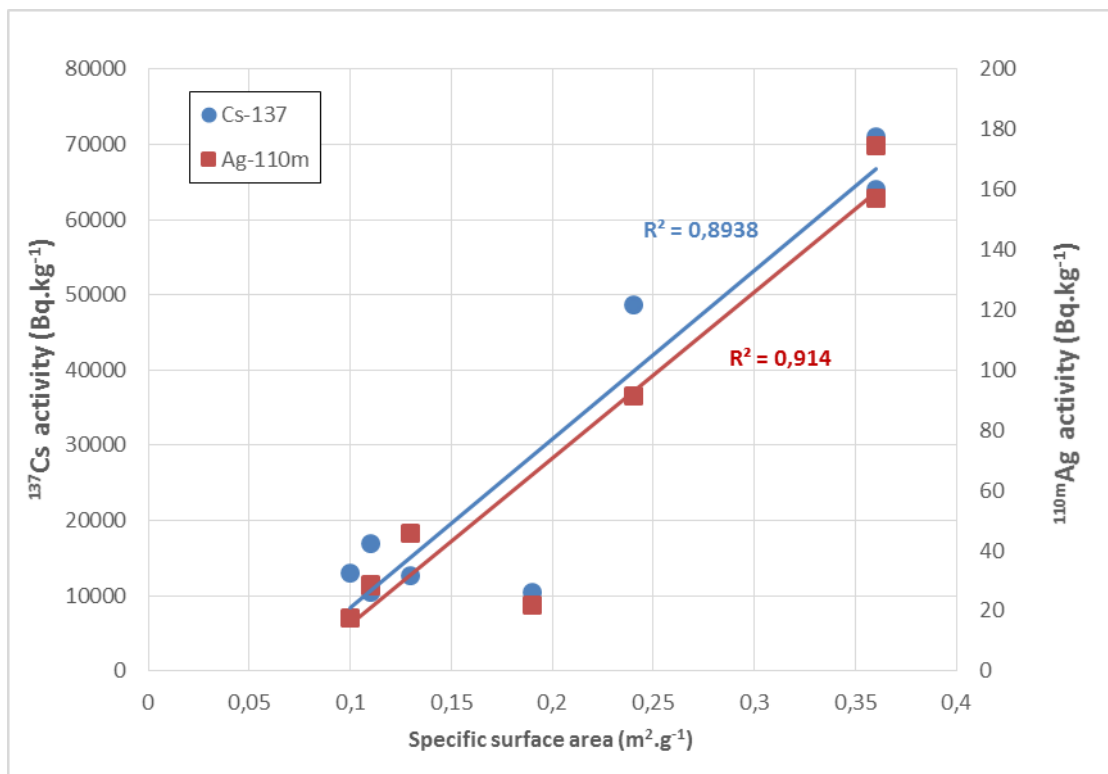


Figure 10



**Table 1**

Literature compilation of radiosilver activities measured in samples collected in the environment in normal and post-accidental conditions.

	Normal conditions				Post-accidental conditions			
	Sample description	Mean (number of samples)	Max	Source	Samples description	Mean (number of samples)	Max	Source
SPM (Bq.kg <sub>dry</sub> <sup>-1</sup> )	Routine monitoring in France (from 2009 to 2012)	<2 (893)	28	(T.Boissieux, IRSN/LS3E, personal communication)	Not investigated to our knowledge			
	Rhone River, France (from 2005 to 2008)	1 ( $\approx$ 10)	<10	Eyrolle et al. (2012)				
Sediment (Bq.kg <sub>dry</sub> <sup>-1</sup> )	Routine monitoring in France (from 2009 to 2012) (Bottom sediment)	<1 (279)	<2.75	(T.Boissieux, IRSN/LS3E, personal communication)	In Fukushima Prefecture (14 March 2011) (Sediment drape deposits)	2 – 2390 (162)	2390	Chartin et al. (2013)
Soil (Bq.kg <sub>dry</sub> <sup>-1</sup> )	Not reported in the literature				In Fukushima Prefecture (11 March 2011)	280 (7)	520	Tazoe et al. (2012)
					In Miyagi Prefecture (26 April 2011)	12 (15)	49	Wanatabe et al. (2012)

SPM : Suspended Particulate Matters

LS3E: Laboratoire de Surveillance de l'Environnement et d'Expertise par Echantillonnage

FDNPP : Fukushima Dai-ichi Nuclear Power Plant

**Table 2.**

Date of collection and location of the samples collected in the framework of this study.

Sample	Date of collection	(WGS 1984):	Latitude	Longitude	Experiment
Soil 1	09/11/2012		37.732447	140.688330	1
Soil 2	10/11/2012		37.567039	140.877110	1
Soil 3	10/11/2012		37.602735	140.994663	1
Soil 4	10/11/2012		37.755403	140.916649	1
Profile	04/2012		37.598136	140.673917	2
Dam Sed 1 (Tetsuzen)	10/11/2012		37.569687	140.879102	3
Dam Sed 2 (Takanokura)	08/11/2012		37.626889	140.882307	3
SDD 1	See Table 7		37.690509	140.676251	4
SDD 2	See Table 7		37.664095	140.778413	4
SDD 3	See Table 7		37.662099	140.728151	4
SDD 4	See Table 7		37.621797	140.695852	4

SDD: Sediment Drape Deposit

**Table 3.**

Distribution of radionuclide activities ( $\text{Bq} \cdot \text{kg}^{-1}$ ) and weight in four grain size fractions of five soils collected across Fukushima radioactive pollution plume. Total activity ( $\text{Bq} \cdot \text{kg}^{-1}$ ) is also given for the bulk sample.

Sample	500 $\mu\text{m} < d < 1000 \mu\text{m}$			250 $\mu\text{m} < d < 500 \mu\text{m}$			63 $\mu\text{m} < d < 250 \mu\text{m}$			d < 63 $\mu\text{m}$			Bulk sample activity	
	Weight (%)	$^{137}\text{Cs}$	$^{110}\text{mAg}$	Weight (%)	$^{137}\text{Cs}$	$^{110}\text{mAg}$	Weight (%)	$^{137}\text{Cs}$	$^{110}\text{mAg}$	Weight (%)	$^{137}\text{Cs}$	$^{110}\text{mAg}$	$^{137}\text{Cs}$	$^{110}\text{mAg}$
Soil 1	8*	21 166 ± 50**	83 ± 36	16	25 636 ± 56	116 ± 40	42	33 682 ± 64	145 ± 44	32	39 490 ± 90	175 ± 62	n/a	n/a
Soil 2	11	929 ± 14	< 14	14	5009 ± 32	< 26	27	14 600 ± 80	93 ± 64	29	19 608 ± 66	179 ± 54	9912 ± 64	98 ± 52
Soil 3	8	298 ± 8	< 10	14	425 ± 14	< 10	35	446 ± 10	< 12	39	580 ± 16	< 8	506 ± 12	< 12
Soil 4	17	576 ± 12	< 14	12	787 ± 14	< 16	34	665 ± 12	< 14	37	1484 ± 26	27 ± 25	634 ± 26	< 22

d: diameter

n/a: not available

\* The remainder of the sample mass correspond to the gravel fraction (>1000  $\mu\text{m}$ )

\*\* Uncertainties on results were estimated by combining counting statistics and calibration uncertainties. Summing and self-absorption effects were taken into account by analysing standards with similar densities and characteristics as the collected samples.

**Table 4.**

Depth distribution of  $^{137}\text{Cs}$  and  $^{110\text{m}}\text{Ag}$  concentrations in the soil profile.

Depth (mm)	$^{137}\text{Cs}$ (Bq.kg $^{-1}$ )	$^{110\text{m}}\text{Ag}$ (Bq.kg $^{-1}$ )	Dry bulk density (g.cm $^{-3}$ )	Mass depth (kg.m $^{-2}$ )
0 – 2	44 698 $\pm$ 74	100 $\pm$ 34	0.19	0.4
2 – 4	47 189 $\pm$ 72	109 $\pm$ 34	0.40	1.2
4 – 6	49 254 $\pm$ 76	101 $\pm$ 38	0.87	2.9
6 – 8	38 335 $\pm$ 64	84 $\pm$ 32	0.73	4.4
8 – 10	31 776 $\pm$ 58	97 $\pm$ 28	0.89	6.2
10 – 12	22 393 $\pm$ 54	32 $\pm$ 24	0.73	7.6
12 – 14	12 575 $\pm$ 38	32 $\pm$ 18	0.92	9.5
14 – 16	7374 $\pm$ 28	20 $\pm$ 14	0.56	10.6
16 – 18	4439 $\pm$ 22	< 12	1.19	13.0
18 – 20	1674 $\pm$ 14	< 16	0.94	14.9
20 - 22	1241 $\pm$ 22	< 16	0.86	16.6

**Table 5.**

Depth, radionuclide activities and grain size proportions of the sequence of sediment accumulated behind Tetsuzen Dam (Ota River)

Depth (cm)	Radionuclide activities and activity ratio			Grain size proportions			
	$^{137}\text{Cs}$ (Bq.kg $^{-1}$ )	$^{110\text{m}}\text{Ag}$ (Bq.kg $^{-1}$ )	$^{110\text{m}}\text{Ag} : ^{137}\text{Cs}$	Clay (%)	Silt (%)	Sand (%)	Gravel (%)
0 - 10	64 195 ± 210	649 ± 142	0.010 ± 0.002	6	62	31	0
10 - 20	165 217 ± 280	1813 ± 196	0.011 ± 0.001	7	58	35	0
20 - 40	1790 ± 24	< 20	n/a	2	3	85	11
40 - 70	146 ± 8	< 18	n/a	5	53	41	2
70 - 85	68 ± 8	< 22	n/a	n/a	n/a	n/a	n/a
85 - 100	33 ± 8	< 40	n/a	5	57	38	0
100 - 110	147 ± 20	< 68	n/a	4	26	45	25
110 - 140	26 ± 4	< 14	n/a	n/a	n/a	n/a	n/a
140 - 162	77 ± 10	< 18	n/a	n/a	n/a	n/a	n/a

n/a: not available

**Table 6.**

Depth, radionuclide activities and grain size proportions of the sequence of sediment accumulated behind Takanokura Dam (Nitta River).

Depth (cm)	Radionuclide activities ( $\text{Bq} \cdot \text{kg}^{-1}$ )		$^{110\text{m}}\text{Ag} : {}^{137}\text{Cs}$	Grain size proportions			
	${}^{137}\text{Cs}$	${}^{110\text{m}}\text{Ag}$		Clay (%)	Silt (%)	Sand (%)	Gravel (%)
0 - 2	$28\ 744 \pm 120$	$246 \pm 88$	$0.0085 \pm 0.0030$	8	56	36	0
2 - 5	$967 \pm 30$	< 32	n/a	5	34	59	2
5 - 20	$616 \pm 18$	< 18	n/a	5	67	28	0
20 - 27	$28 \pm 4$	< 12	n/a	8	48	44	0
27 - 35	$728 \pm 16$	< 18	n/a	7	63	29	0
35 - 40	$592 \pm 10$	< 12	n/a	8	44	48	1
40 - 50	$124 \pm 6$	< 16	n/a	7	49	42	2

n/a: not available

**Table 7.**

Characteristics of the riverbed sediment from the upper part of the Nitta River catchment collected at the same locations during the three fieldwork campaigns.

Sample	Sampling date	$^{137}\text{Cs}$ activity (Bq.kg $^{-1}$ )	$^{110\text{m}}\text{Ag}$ activity (Bq.kg $^{-1}$ )	$^{110\text{m}}\text{Ag} : ^{137}\text{Cs}$	SSA (m $^2\text{.g}^{-1}$ )	pH
SDD 1	Nov-2011	71 014 ± 108	157 ± 30	0.0022 ± 0.0004	0.36	n/a
	Apr-2012	6 939 ± 34	22 ± 16	0.0031 ± 0.0023	n/a	n/a
	Nov-2012	10 394 ± 62	< 38	n/a	0.19	6 ± 0.5
SDD 2	Nov-2011	10 385 ± 32	29 ± 10	0.0028 ± 0.0010	0.11	n/a
	Apr-2012	13 885 ± 34	23 ± 18	0.0016 ± 0.0013	n/a	n/a
	Nov-2012	12 583 ± 48	46 ± 34	0.0036 ± 0.0027	0.13	6 ± 0.5
SDD 3	Nov-2011	16 898 ± 66	29 ± 22	0.0017 ± 0.0013	0.11	n/a
	Apr-2012	337 786 ± 72	132 ± 34	0.0035 ± 0.0009	n/a	n/a
	Nov-2012	48 680 ± 178	92 ± 55	0.0019 ± 0.0011	0.24	5.5 ± 0.5
SDD 4	Nov-2011	64 093 ± 100	175 ± 16	0.0027 ± 0.0002	0.36	n/a
	Apr-2012	65 599 ± 106	161 ± 24	0.0024 ± 0.0004	n/a	n/a
	Nov-2012	12 949 ± 74	< 44	n/a	0.1	6

n/a: not available

**Table 8**

Comparison of  $^{110m}\text{Ag}$ : $^{137}\text{Cs}$  activity ratio between soil and sediment drape deposits collected during the three campaigns in the upper part of the Nitta River catchment. All values were decay-corrected to 14 march 2011.

---

$^{110m}\text{Ag}$ : $^{137}\text{Cs}$ activity ratio	Soil (based on MEXT data)	SDD
Nov-11	$0.0023 \pm 0.008$	$0.0023 \pm 0.0005$
Apr-12		$0.0027 \pm 0.0008$
Nov-12		$0.0022 \pm 0.0010$

---

SDD: Sediment Drape Deposits